Supplementary Information (SI) for ChemComm.
This journal is © The Royal Society of Chemistry 2025

Supporting Information

Side chain polymerization for non-conjugated polymer acceptor

Haotian Wu,[a] Kai Xiang,[a] Yirong Li,[a] Mengran Peng,[a] Jianhua Chen, *[a] Hao Xia, *[b] Ning Su,*[a] Yongqiang Shi*[c]

[a] Key Laboratory of Medicinal Chemistry for Natural Resource, Ministry of Education. School of Chemical Science and Technology, Yunnan University, Kunming 650091, China.

[b] Department of Electrical and Electronic Engineering, Research Institute of Smart Energy (RISE), Photonic Research Institute (PRI), The Hong Kong Polytechnic University, Hung Hum Kowloon, Hong Kong, China.

[c] Key Laboratory of Functional Molecular Solids, Ministry of Education, and Anhui Key Laboratory of Molecule-Based Materials and Anhui Key Laboratory of Biomedical Materials and Chemical Measurement, School of Chemistry and Materials Science, Anhui Normal University, Anhui, 241002, China.

1. General Information

To explore potential packing configurations of SPA-1 and corresponding PSMA-type main chain polymer acceptor, molecular docking simulations[1] were carried out using the GFN-FF force field[2] implemented in the xtb[3] program. The resulting structures were subsequently fully optimized with GFN-FF to identify stable interaction geometries.

All reactions were conducted under the nitrogen atmosphere, and all the starting materials and solvents were obtained from commercial suppliers and utilized without additional purification. PBDB-T, PM6 and PY-IT were purchased from Derthon Optoelectronic Materials Science Technology, Ag (99.999%) and other materials for the fabrication of device were purchased from Alfa, Aldrich. The synthetic route to grafted non-conjugated polymer acceptor SPA-1 is shown in Fig. S2.

The ^1H and ^{13}C NMR spectra were acquired on a Bruker AVANCE III 400 MHz spectrometer at room temperature with using deuterated $CDCl_3$ as solvent and tetramethyl silane (TMS) as reference. Mass spectra were measured on a Bruker Daltonics RAPIFLEX MALDI-TOF analyzer under MALDI mode. The average number (Mn) and weight (Mw) molecular weight and polydispersity index (PDI) of the non-conjugated polymer acceptor SPA-1 were obtained by a SHIMADZU RID-20A gel permeation chromatography (GPC) at 35 °C, using tetrahydrofuran as an eluent.

Thermogravimetric Analysis (TGA) were conducted on a Shimazu DTG-60A differential thermal thermogravimetric synchronization analyzer, with a scanning rate of 10 °C min^{-1} over the temperature range of 40 to 600 °C. Differential scanning calorimetry (DSC) thermograms were obtained by using a Q-200 calorimeter (TA instruments, USA) with the heating rate of 10 °C min^{-1} over the temperature range of 20–280 °C.

UV-Vis absorption spectra were recorded on a UV-3600i Shimadzu UV-visible-near-infrared spectrophotometer over the wavelength range of 280-1000 nm.

Photoluminescence (PL) spectra were measured on a HORIBA FLUOROMAX_PLUS_P spectrofluorometer, and the excited wavelength were set at

460 nm and at 650 nm.

Cyclic voltammetry (CV) measurements were conducted on a CHI760E A21731 instrument, using a platinum plate as the working electrode, a platinum wire electrode as the counter electrode, and an Ag/AgCl electrode as the reference electrodes, respectively. SPA-1 were drop-cast onto the working electrode from chloroform solutions to form thin films. The measurements were carried out in a deoxygenated, anhydrous 0.1M tetra-n-butylammonium hexafluorophosphate ($TBAPF_6$) acetonitrile solution, and the scan rate was set at 100 mV s^{-1}.

The atomic force microscopy (AFM) images were investigated in a Japanese Seiko SPI-3800 scanning probe microscope.

The optimized PBDB-T:SPA-1 based binary all-polymer solar cells (All-PSCs) were fabricated with a structure of ITO/PEDOT:PSS (30 nm)/Active layers (90 nm)/PFN-Br (5 nm)/Ag (150 nm). The ITO glasses were washed with detergent and then ultrasonic precleaned with deionized water, acetone, and isopropanol, then subsequently dried at 100°C for 1 hour. The ITO glasses were treated with UV-ozone for 30 min before use. PEDOT:PSS (30 nm) (Heraeus Clevios P VP AI 4083) was spin-coating onto the ITO glasses at 3800 rpm for 30 s, and then annealed in an oven at 150 °C for 15 min. Then the device was transferred to a nitrogen glove box. The active layer was spin-coated from 11.25 mg mL^{-1} solution dissolved in chloroform (CF) (PBDB-T:SPA-1 = 1:1.25, PBDB-T = 5.0 mg mL^{-1}, 0.5% v/v DIO) at 2000 rmp for 0.5 min onto the PEDOT:PSS film, and then annealed at 80 °C for 15 min to form a CF treated active layer. The active layer was spin-coated from 22.5 mg mL^{-1} solution dissolved in chlorobenzene (CB) (PBDB-T:SPA-1 = 1:1.25, PBDB-T = 10.0 mg/mL, 0.5% v/v DIO) at 2000 rmp for 0.5 min onto the PEDOT:PSS film, then annealed at 80 °C for 15 min to form a CB treated active layer. In the presence of trace amounts of acetic acid, a thin PFN-Br layer (5 nm) was spun onto the active layer from the methanol solution, followed by the deposition of Ag (150 nm) under 5.0×10^{-4} Pa to accomplish the device fabrication.

The optimized PM6:PY-IT based binary All-PSCs and PM6:PY-IT:SPA-1 based ternary All-PSCs were fabricated with a structure of ITO/2PACZ (5 nm)/Active layers (90 nm)/PDINN (5 nm)/Ag (100 nm). The cleaning steps for ITO glasses are the same as the aforementioned. 2PACZ (5 nm) was spin-coating from 0.3 mg mL^{-1} solution dissolved in ethanol onto the ITO glasses at 3000 rpm for 40 s. Then the device was transferred to a nitrogen glove box. The active layer was spin-coated from 17.6 mg mL^{-1} solution dissolved in chlorobenzene (CB) (PM6:PY-IT = 1:1.2, PM6 = 8.0 mg mL^{-1}, 1% CN) at 2000 rmp for 0.5 min onto the 2PACZ film, then annealed at 100 °C for 5 min to form a PM6:PY-IT based binary active layer. The active layer was spin-coated from 17.6 mg mL^{-1} solution dissolved in chlorobenzene (CB) (PM6:PY-IT:SPA-1 = 1:1.1:0.1, PM6 = 8.0 mg mL^{-1}, 1% CN) at 2000 rmp for 0.5 min onto the 2PACZ film, then annealed at 100 °C for 5 min to form a PM6:PY-IT:SPA-1 based ternary active layer. In the presence of trace amounts of acetic acid, a thin PDINN layer (5 nm) was spun onto the active layer from the methanol solution, followed by the deposition of Ag (100 nm) under 5.0×10^{-4} Pa to accomplish the device fabrication.

An optical microscope (Olympus BX51) was used to define the effective area of one cell (0.059 cm^2). The current density-voltage (*J-V*) curves were measured by a Keithley 2400 Source Meter under AM 1.5G (100 mW cm^{-2}) using a Newport solar simulator. The light intensity was calibrated using a standard Si diode (with KG5 filter, purchased from PV Measurements to bring spectral mismatch to unity). EQEs were measured using an Enlitech QE-S EQE system equipped with a standard Si diode. Monochromatic light was generated from a Newport 300W lamp source.

The electron and hole mobilities were evaluated by the space charge limited current (SCLC) method. The device architecture of the electron-only devices was ITO/ZnO (25 nm)/Active layer (90 nm)/PFN-Br (5 nm)/Ag (100 nm) and that of the hole-only devices was ITO/PEDOT: PSS (30 nm)/Active layer (90 nm)/MoO_3 (10 nm) /Ag (100 nm). The charge carrier mobilities were determined by fitting the dark current into the model of a single carrier SCLC according to the equation:

$$J = \frac{9}{8}\varepsilon_r\varepsilon_0\mu\frac{V^2}{d^3}$$

where J is the current density, ε_r is the dielectric constant of active layer, ε_0 is the vacuum permittivity, μ is the mobility of hole or electron and d is the thickness of the active layer, V is the internal voltage in the device, and $V = V_{appl} - V_{bi}$, where V_{appl} is the voltage applied to the device, and V_{bi} is the built-in voltage resulting from the relative work function difference between the two electrodes.

2. Molecular Dynamics (MD) Simulations.

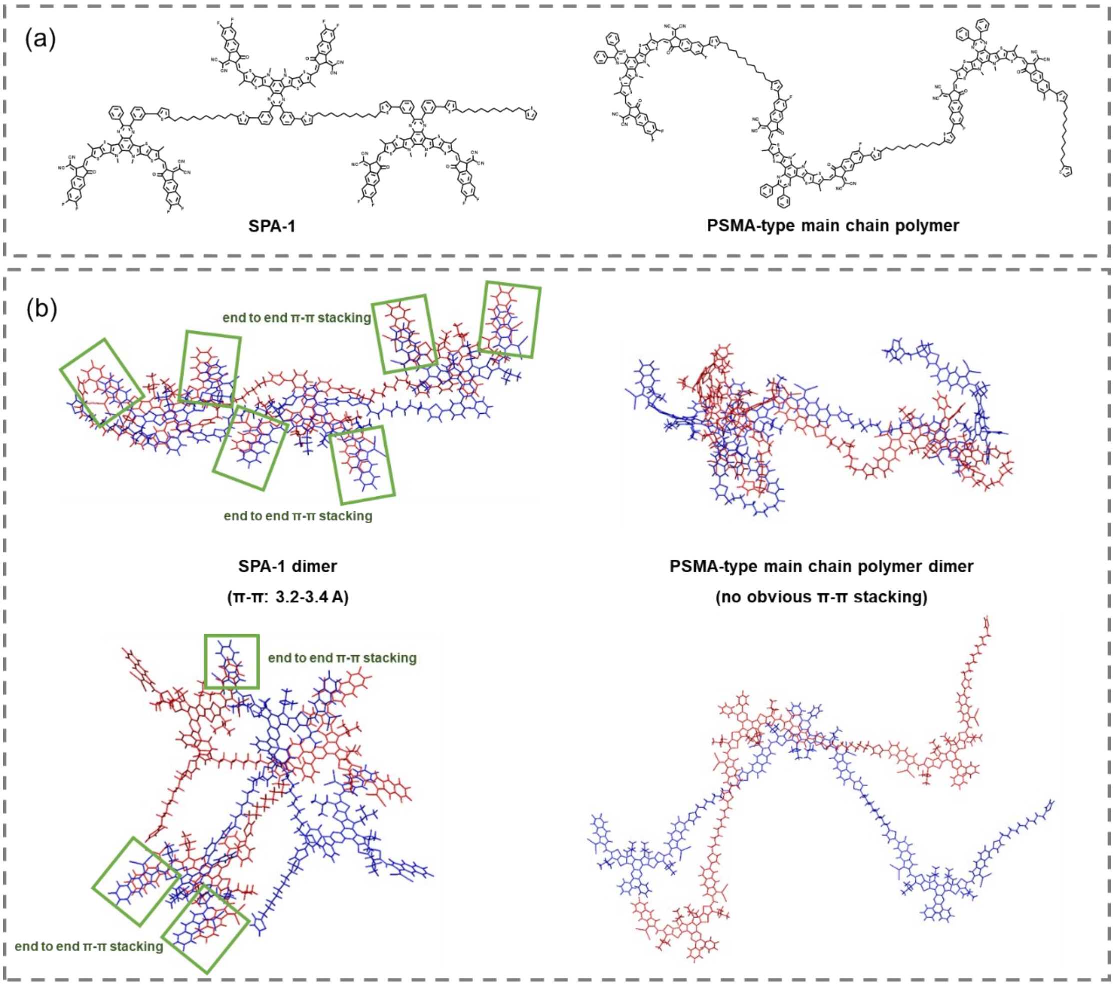

Fig. S1 (a) Chemical structures of SPA-1 and the corresponding PSMA-type main chain polymer (For clarity, only fragments are depicted, and the alkyl side chains are simplified with methyl); (b) Intermolecular interactions and corresponding packing patterns of SPA-1 and the associated PSMA-type main chain polymer as derived from molecular dynamics (MD) simulations.

3. Molecular Synthesis

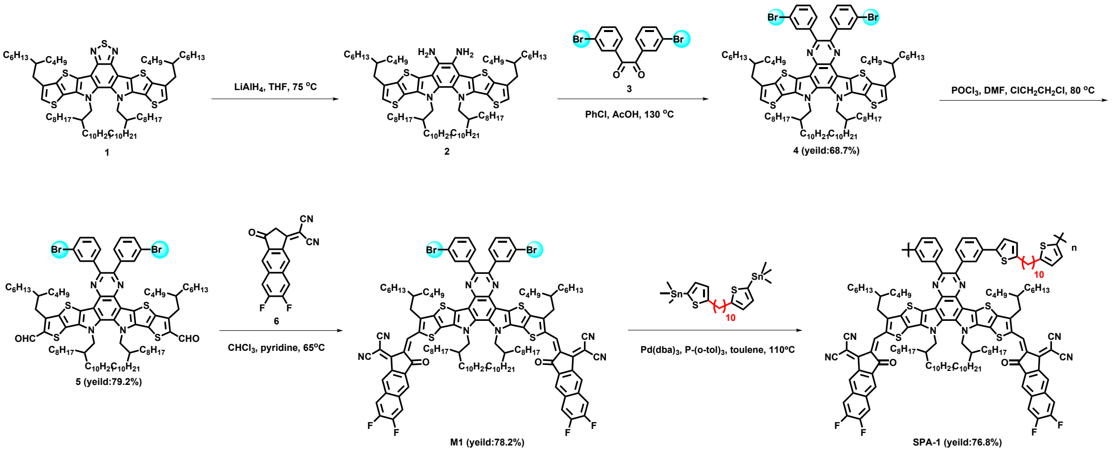

Fig. S2 The synthetic route of SPA-1.

Synthesis of Compound 2. To a 50 mL three-necked round bottom flask, a mixture of compound **1** (500.00 mg, 0.37 mmol, 1.00 eq) and $LiAlH_4$ (282.50 mg, 7.48 mmol, 20.00 eq) was added, anhydrous tetrahydrofuran (20.00 mL) at 0 °C under the protection of nitrogen. The mixture was heated to 75 °C and stirred for 6 h. After cooling to 0 °C, cold brine was added slowly to quench the remaining $LiAlH_4$. The mixture was extracted with ethyl acetate three times. After removal of the solvent, compound **2** (489.50 mg, 0.37 mmol) was obtained and can be used in the next step without further purification.

Synthesis of Compound 4. To a 25 mL three-necked round bottom flask, a mixture of compound **2** (489.50 mg, 0.37 mmol, 1.00 eq) and1,2-bis(3-bromophenyl)ethane-1,2-dione (Compound **3**) (206.50 mg, 0.56 mmol, 1.50 eq) was added, followed by chlorobenzene (7.50 mL) and acetic acid (7.50 mL), then the mixture was heated to 130 °C and stirred overnight under the protection of nitrogen. After cooling to room temperature, the mixture was washed with water, extracted with dichloromethane, and dried with anhydrous $MgSO_4$. The resulting crude product was purified by silica gel column using petroleum ether as the eluent to afford compound **4** as an orange oil (421.30 mg, 69 %). ^1H NMR (400 MHz, Chloroform-d) δ (ppm): 8.11 (d, J = 2.0 Hz, 2H), 7.60 (d, J = 7.7 Hz, 2H), 7.55 (dd, J = 8.0, 2.1 Hz, 2H), 7.24 (d, J = 7.8 Hz, 2H), 6.99 (s, 2H), 4.67 (d, J = 7.7 Hz, 4H), 2.78 (d, J = 7.1 Hz, 4H), 2.20–1.98 (m, 4H), 1.50–0.64 (m, 134H). ^{13}C NMR (101 MHz, Chloroform-d) δ (ppm): 147.15, 143.82, 141.96, 137.83, 136.18, 134.18, 133.41, 131.45, 131.35, 129.65, 129.20, 123.54, 122.58, 122.31, 119.90, 117.57, 55.21, 38.73, 37.51, 34.64, 33.89, 33.54, 32.07, 32.04, 31.95, 30.58, 29.90, 29.83, 29.71, 29.63, 29.52, 29.46, 29.27, 28.99, 26.73, 25.68, 23.24, 22.85, 22.75, 14.35, 14.28, 14.24. MS (MALDI-TOF) m/z calcd. for $C_{96}H_{142}Br_2N_4S_4$ $[M+H]^+$: 1638.8464; found, 1638.8101.

Synthesis of Compound 5. To a 100 mL three-necked round bottom flask, $POCl_3$ (1.28 mL) and *N, N*-dimethylformamide (7.26 mL) were added under the protection of nitrogen, and the solution was stirred at 0 °C for 2 h. Then, compound **4** (400.00 mg, 0.24 mmol) dissolved in 1,2-dichloroethane solution (40.00 mL) was added, then the mixture was heated to 80 °C and stirred for 6 h. After cooling to room temperature, the mixture was quenched with saturated sodium acetate solution and extracted with dichloromethane. The organic phase was evaporated, and the residue was purified by silica gel column using a mixture of petroleum/dichloromethane (*v/v* = 4:1) as the eluent to afford compound **5** as an orange oil (327.90 mg, 79%). ^1H NMR (400 MHz, Chloroform-d) δ (ppm): 10.13 (s, 2H), 8.12 (t, *J* = 1.8 Hz, 2H), 7.57 (dd, *J* = 8.0, 6.6, 1.7 Hz, 4H), 7.25 (d, *J* = 7.8 Hz, 2H), 4.69 (d, *J* = 7.9 Hz, 4H), 3.14 (d, *J* = 7.4 Hz, 4H), 2.13 (h, *J* = 6.2, 5.6 Hz, 4H), 1.49–0.70 (m, 128H). ^{13}C NMR (101 MHz, Chloroform-d) δ (ppm): 182.16, 148.26, 146.67, 144.77, 141.42, 137.78, 137.51, 134.45, 133.35, 132.47, 131.87, 129.75, 129.61, 129.08, 127.21, 122.76, 118.31, 55.48, 39.34, 38.99, 34.00, 33.64, 33.21, 32.02, 31.97, 31.91, 30.59, 29.81, 29.78, 29.68, 29.62, 29.46, 29.43, 29.40, 29.27, 28.92, 26.73, 25.68, 23.13, 22.81, 22.78, 22.72, 14.25, 14.22. MS (MALDI-TOF) m/z calcd. for $C_{96}H_{142}Br_2N_4O_2S_4$ $[M+H]^+$: 1694.8362; found, 1694.8137.

Synthesis of Compound M1. To a 100 mL three-necked round bottom flask, dry pyridine (3.00 mL) was added to a solution of compound **5** (300.00 mg, 0.18 mmol, 1.00 eq) and 2-(6,7-difluoro-3-oxo-2,3-dihydro-1H-cyclopenta[b]naphthalen-1-ylidene)malononitrile (compound **6**) (297.40 mg, 1.06 mmol, 6.00 eq) in chloroform (65.00 mL) under the protection of nitrogen. The resulting mixture was stirred and heated to reflux for 12 h. After cooling to room temperature, the solvent was removed under vacuum. The crude product was settled in methanol and filtered out, then purified by column chromatography on silica gel with a mixture of petroleum /chloroform (v/v = 3:1) as eluent to afford compound M1 as a black solid (307.50 mg, 78 %). ^{1}H NMR (400 MHz, Chloroform-d) δ (ppm): 9.23 (s, 2H), 9.10 (s, 2H), 8.32 (s, 2H), 8.10 (t, J = 1.9 Hz, 2H), 7.80 (dt, J = 9.9, 7.6 Hz, 4H), 7.59 (dd, J = 11.3, 7.5, 1.9 Hz, 4H), 7.29 (d, J = 7.9 Hz, 2H), 4.87 (d, J = 7.9 Hz, 4H), 3.22 (d, J = 7.5 Hz, 4H), 2.34–2.03 (m, 4H), 1.51–0.69 (m, 131H). ^{13}C NMR (101 MHz, Chloroform-d) δ (ppm): 187.70, 160.33, 153.93, 148.84, 146.79, 140.85, 138.36, 136.35, 136.14, 135.39, 134.97, 134.64, 133.54, 133.44, 133.12, 132.47, 132.04, 130.97, 129.74, 128.86, 125.40, 122.72, 121.98, 119.39, 115.98, 115.56, 66.81, 55.80, 40.15, 39.23, 34.53, 33.58, 33.27, 31.95, 31.89, 30.65, 29.92, 29.75, 29.70, 29.66, 29.51, 29.45, 29.42, 29.30, 28.85, 26.64, 25.79, 23.00, 22.69, 14.17, 14.13. MS (MALDI-TOF) m/z calcd. for $C_{130}H_{150}Br_2N_8F_4O_2S_4$ [M+H]$^+$: 2220.9078; found, 2220.9068.

Synthesis of non-conjugated polymer acceptor SPA-1. M1 (110.00 mg, 0.05 mmol, 1.00 eq), 1,10-bis(5-(trimethyltin)thiophen-2-yl)decane (31.60 mg, 0.05 mmol, 1.00 eq), $Pd_2(dba)_3$ (5.00 mg) and $P(o\text{-}tol)_3$ (13.30 mg) were combined in a 10 mL two-necked flask, then anhydrous toluene (2.50 mL) was added under the argon atmosphere. The mixture was stirred at 110 °C for 24 h. After cooling to room temperature, the resulting mixture was poured into methanol. The precipitate was filtered and Soxhlet extracted with methanol, acetone, hexane, and chloroform sequentially. The extracted solution was concentrated and precipitated into 100 mL methanol, filtered and dried under vacuum to afford SPA-1 as a black solid (87.10 mg, 77%). ^{1}H NMR (400 MHz, Chloroform-d) δ (ppm): 9.29–8.90 (m, 4H), 8.19 (s, 3H), 7.97–7.32 (m, 12H), 7.14–6.91 (m, 2H), 6.77–6.56 (m, 2H), 4.91 (br, 4H), 3.04 (br, 4H), 2.78 (m, 4H), 2.34 (br, 2H), 2.00 (br, 2H), 1.80–1.56 (m, 7H), 1.51–0.62 (m, 148H).

4. Thermal Performance Analysis

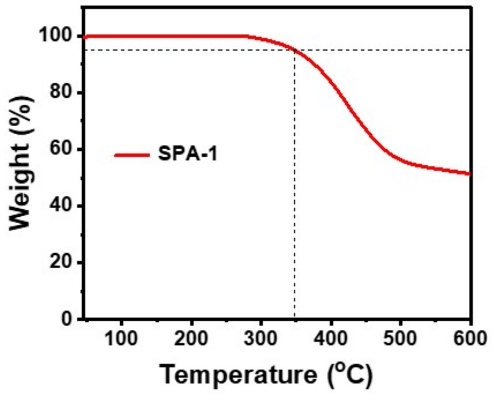

Fig. S3 The TGA curves of SPA-1.

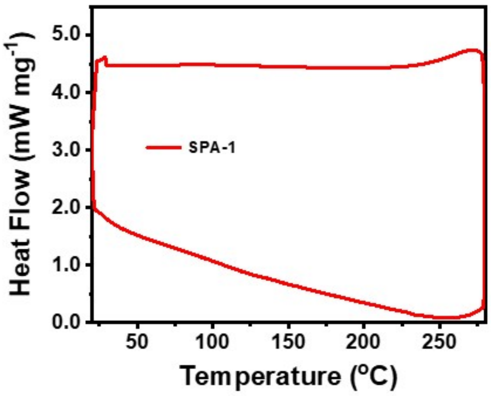

Fig. S4 The DSC curves of SPA-1.

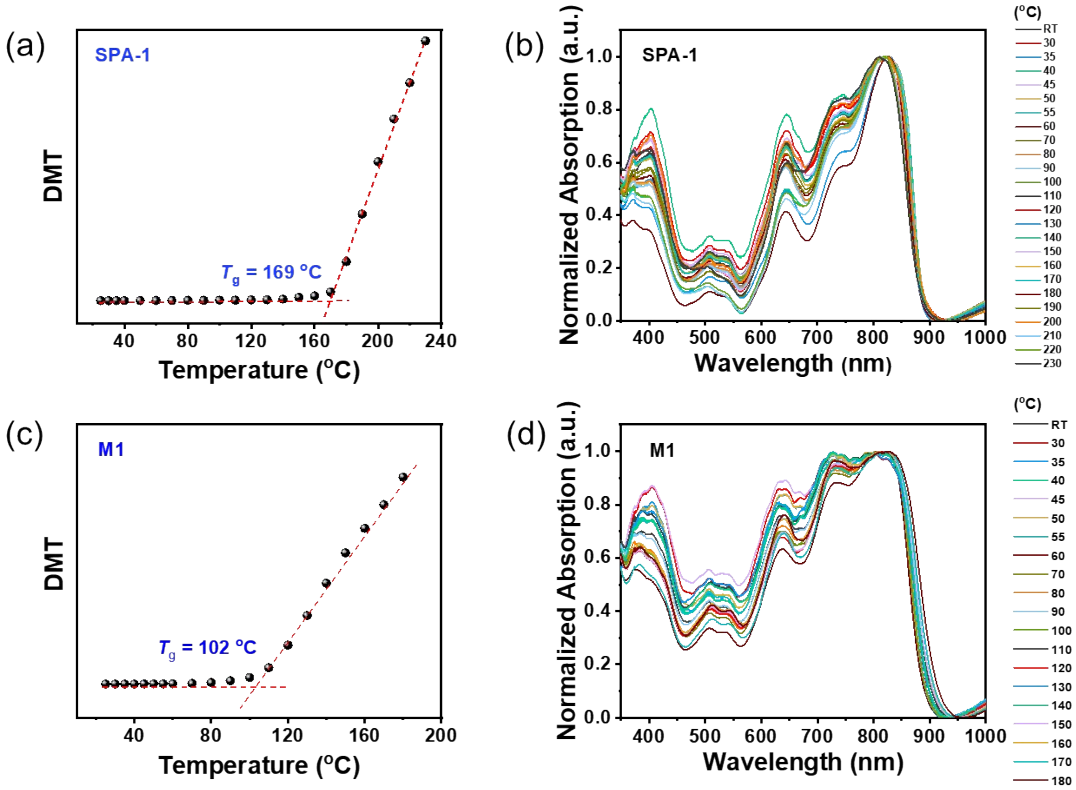

Fig. S5 (a) The measurement of T_g by fitting UV-vis deviation metric results; (b) Normalized absorption spectra of SPA-1 neat film after thermal annealing at different temperatures for 2 minutes; (c) The measurement of T_g by fitting UV-vis deviation metric results and (d) Normalized absorption spectra of M1 neat film after thermal annealing at different temperatures for 2 minutes.

5. UV-Vis Absorption Spectra of SPA-1 and M1

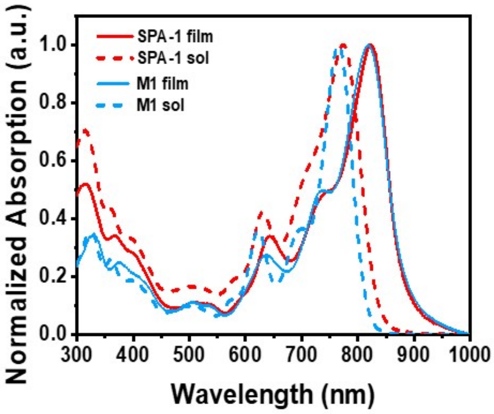

Fig. S6 The UV-Vis absorption spectral of SPA-1 and M1 in the dilute chloroform solution and the thin-film state.

6. Electrochemical Cyclic Voltammetry (CV) Curves

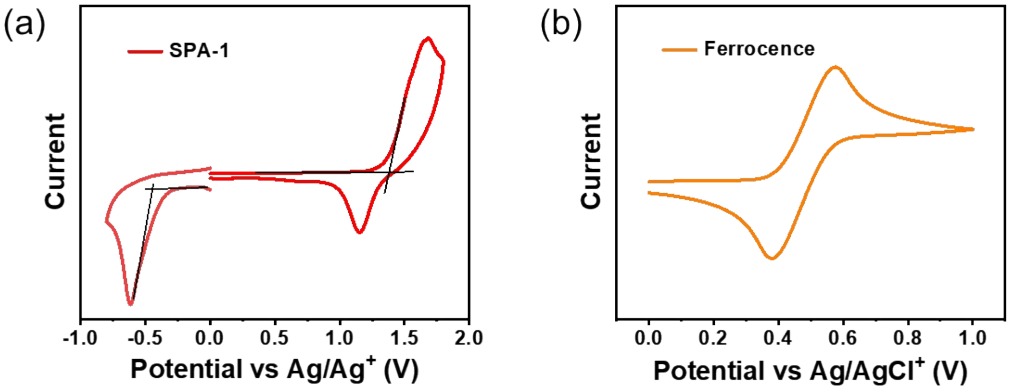

Fig. S7 The cyclic voltammetry curves of (a) SPA-1 and (b)electrochemical redox pattern of ferrocene. The LUMO and HOMO energy levels are calculated from the formula: $E_{HOMO/LUMO} = -[\Phi_{ox/red}-\Phi_{Fc/Fc+}+4.8]$ eV.

7. Binary All-PSCs Device Structure and Optimization Process

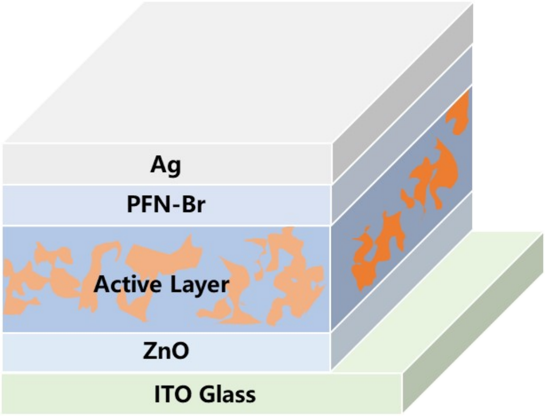

Fig. S8 The device structure of the PBDB-T:SPA-1 based binary All-PSCs.

Table S1. Photovoltaic parameters of the binary All-PSCs based on SPA-1 under AM 1.5G irradiation (100 mW cm^{-2}).

Donor	Donor concentration and solvent	D:A	Additive	Treatment	Speed (rmp)	V_{OC} (V)	J_{SC} (mA cm^{-2})	FF (%)	PCE (%)
PM6	5 mg mL^{-1} in CF	1:1.25	1%CN	As cast	2000	0.926	9.45	65.08	5.67
PM7	5 mg mL^{-1} in CF	1:1.25	1%CN	As cast	2000	0.910	4.44	58.90	2.38

D18	5 mg mL^{-1} in CF	1:1.25	1%CN	As cast	2000	0.910	5.35	56.08	2.73
PBDB-T	5 mg mL^{-1} in CF	1:1.25	1%CN	As cast	2000	0.831	17.60	64.12	9.38
PBDB-T	5 mg mL^{-1} in CF	1:1.00	1%CN	As cast	2000	0.838	16.79	65.45	9.21
PBDB-T	5 mg mL^{-1} in CF	1:1.50	1%CN	As cast	2000	0.828	15.81	61.86	8.10
PBDB-T	5 mg mL^{-1} in CF	1.1.75	1%CN	As cast	2000	0.809	14.52	59.38	6.99
PBDB-T	10 mg mL^{-1} in CB	1:1.25	DIB	TA 80 ℃ 15 min	2000	0.861	20.28	60.74	10.61
PBDB-T	10 mg mL^{-1} in CB	1:1.25	DIB	TA 80 ℃ 15 min	2500	0.863	18.48	63.29	10.05
PBDB-T	10 mg mL^{-1} in CB	1:1.25	DIB	TA 80 ℃ 15 min	3000	0.863	17.06	62.60	9.23
PBDB-T	10 mg mL^{-1} in CB	1:1.25	DIB	SVA 30 s + TA	2000	0.865	17.09	65.04	9.62
PBDB-T	10 mg mL^{-1} in CB	1:1.25	DIB	SVA 60 s + TA	2000	0.856	17.53	64.31	9.66
PBDB-T	10 mg mL^{-1} in CB	1:1.25	DIB	SVA 90 s + TA	2000	0.861	18.02	61.05	9.48
PBDB-T	10 mg mL^{-1} in CB	1:1.25	DIB	SVA 120 s + TA	2000	0.860	19.96	58.49	10.04
PBDB-T	10 mg mL^{-1} in CB	1:1.25	0.5%DIO	TA 80 ℃ 15 min	2000	0.857	21.29	61.16	11.16
PBDB-T	10 mg mL^{-1} in CB	1:1.25	0.5%DIO	As cast	2000	0.867	19.29	61.40	10.27
PBDB-T	5 mg mL^{-1} in CF	1:1.25	0.5%DIO	TA 80 ℃ 15 min	2000	0.820	19.17	62.64	9.85

8. Photovoltaic Performance Comparison

Table S2. Photovoltaic parameters for the A-D-A and A-DA’D-A type non-conjugated copolymer/terpolymer acceptors containing binary all-polymer solar cells.

Donor	Non-conjugated copolymer acceptors	Non-conjugated terpolymer acceptors	V_{OC} (V)	J_{SC} (mA cm^{-2})	FF (%)	PCE (%)	References
PBDB-T	PYT8T	/	0.950	17.01	62.00	9.97	[4]
PBDB-T	PFY-2TS	/	0.906	20.47	66.30	12.31	[5]
D18	NC-PY6	/	0.870	20.66	68.42	12.30	[6]
JD40	PJTET	/	0.920	18.58	63.84	10.93	[7]
PBDB-T	PTH-Y	/	0.956	12.01	57.20	6.59	[8]
PBDB-T	PTCl$_m$-Y	/	0.941	15.86	55.30	8.25	[8]
PBDB-T	PTCl$_o$-Y	/	0.948	20.21	66.50	12.47	[8]
PBDB-T	PYTS-1.0	/	0.890	4.31	44.00	1.71	[9]
PBDB-T	PYTS-C2	/	0.910	19.15	66.00	11.37	[10]
PBDB-T	PYTS-C4	/	0.900	8.53	47.00	3.73	[10]
PBDB-T	PYTS-C8	/	0.920	6.65	47.00	2.97	[10]
PM6	PY-IF1	/	0.887	20.49	64.56	11.73	[11]
PM6	PYFTET-L	/	0.970	18.16	54.30	9.53	[12]
PM6	PYFTET-H	/	0.960	17.12	50.90	8.27	[12]
PM6	PF1-TS4	/	0.980	15.04	58.50	8.63	[13]
PBDB-T	/	PYFS-Ran	0.920	20.93	64.00	12.16	[4]
PBDB-T	/	PYFS-Reg	0.920	23.52	74.00	16.09	[4]
PBDB-T	/	PYTS-0.1	0.920	22.52	68.00	14.19	[9]
PBDB-T	/	PYTS-0.3	0.920	22.91	70.00	14.68	[9]
PBDB-T	/	PYTS-0.5	0.920	14.46	60.00	7.91	[9]
PM6	/	PYF1-A	0.941	21.62	66.91	13.60	[11]
PM6	/	PYF1-B	0.947	23.21	74.01	16.27	[11]
PM6	/	PYTH-A	0.943	22.89	71.28	15.39	[14]
PM6	/	PYTCl-A	0.942	23.49	73.04	16.16	[14]
PM6	/	PYTH-B	0.937	20.35	68.78	13.12	[14]
PM6	/	PYTCl-B	0.935	20.76	70.14	13.61	[14]
PBDB-T	/	PYSe-TC6T(5)	0.882	22.82	64.29	12.94	[15]
PBDB-T	/	PYSe-TC6T(10)	0.891	22.94	66.26	13.54	[15]

PBDB-T	/	PYSe-TC6T(20)	0.906	20.08	62.66	11.40	[15]
PBDB-T	/	PYSiO-5	0.920	20.60	60.00	11.40	[16]
PBDB-T	/	PYSiO-10	0.920	21.62	67.00	13.52	[16]
PBDB-T	/	PYSiO-20	0.910	20.68	64.00	11.94	[16]
PBDB-T	/	PYSiO-30	0.920	19.40	60.00	10.74	[16]
PM6	/	PF1-TS4-20	0.990	13.73	59.70	8.12	[17]
PM6	/	PF1-TS4-40	0.990	14.67	60.80	8.83	[17]
PM6	/	PF1-TS4-60	0.990	15.30	61.40	9.31	[17]
PM6	/	PF1-TS4-80	0.970	15.51	60.30	9.16	[17]
PM6	/	J1	0.910	22.61	77.60	15.89	[18]
PM6	/	J2	0.880	23.47	79.70	16.48	[18]
PM6	/	J3	0.870	23.45	77.70	15.85	[18]
PBDB-T	SPA-1	/	0.871	21.30	61.16	11.16	This work

9. Ternary All-PSCs

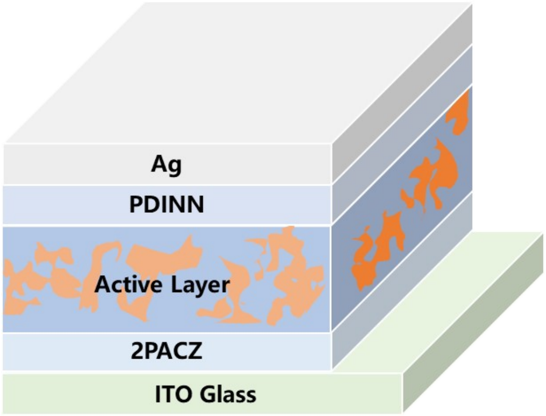

Fig. S9 The device structure of the PM6:PY-IT based binary All-PSCs and PM6:PY-IT:SPA-1 based ternary All-PSCs.

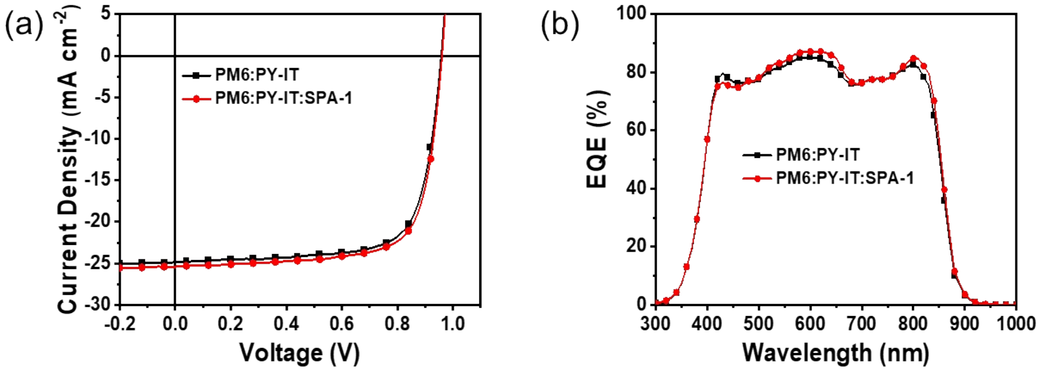

Fig. S10 (a) *J-V* curves and (b) EQE spectra of the PM6:PY-IT based binary All-PSCs and PM6:PY-IT:SPA-1 based ternary All-PSCs.

Table S3. Photovoltaic parameters of the PM6:PY-IT based binary All-PSCs and PM6:PY-IT:SPA-1 based ternary All-PSCs.

Device	V_{OC}	J_{SC}	J_{cal}[b]	FF	PCE[a]
	(V)	(mA cm^{-2})	(mA cm^{-2})	(%)	(%)
PM6:PY-IT	0.955	24.89	24.03	73.13	17.40 (17.11±0.35)
PM6:PY-IT:SPA-1	0.960	25.40	24.45	73.36	17.91 (17.66±0.26)

[a] The data in brackets are the average values at least 10 independent devices for each blend. [b] Obtained from the integration of EQEs with AM1.5G spectrum.

10. UV-Vis Absorption Spectra and Photoluminescence (PL) Spectra for Blend Films

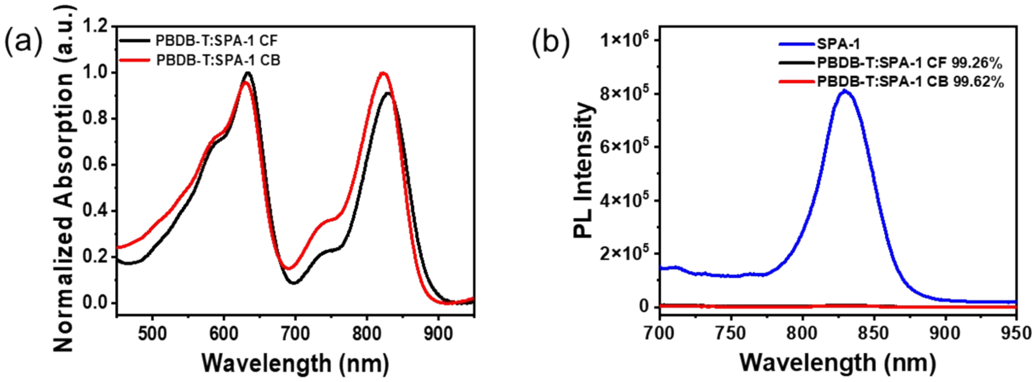

Fig. S11 (a) UV-vis absorption spectral of PBDB-T:SPA-1 blend films treated with CF or CB and (b) PL spectral of PBDB-T neat film and PBDB-T:SPA-1 blend films treated with CF or CB excited at 650 nm.

11. Space Charge Limited Current (SCLC) Measurement

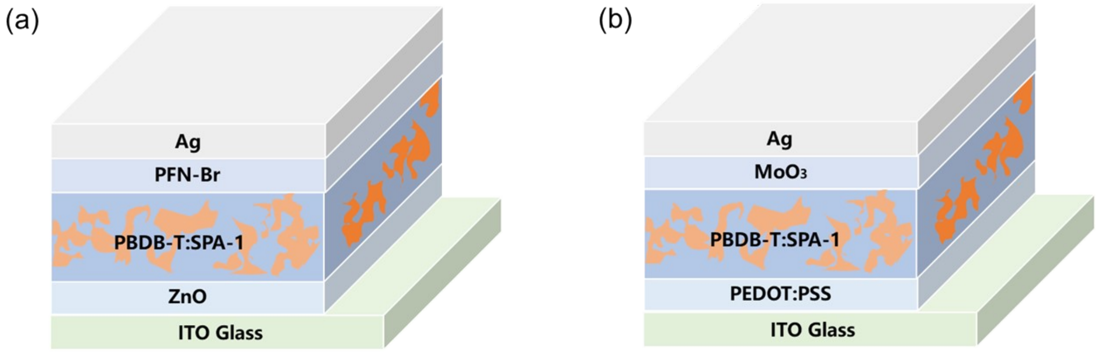

Fig. S12 The device structure of (a) the electron-only devices and (b) the hole-only devices.

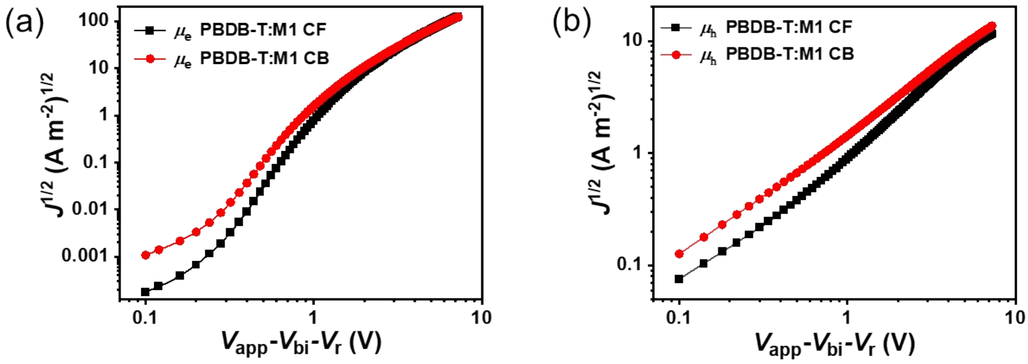

Fig. S13 (a) Electron mobilities and (b) hole mobilities of the PBDB-T:M1 based OSCs treated with CF or CB.

Table S4. The electron and hole mobilities of the PBDB-T:SPA-1 based binary All-PSCs and PBDB-T:M1 based binary OSCs.

Device	μ_e (cm^2 V^{-1} s^{-1})	μ_h (cm^2 V^{-1} s^{-1})	μ_e /μ_h
PBDB-T:SPA-1 (CF treated)	1.20×10^{-4}	6.40×10^{-5}	1.88
PBDB-T:SPA-1 (CB treated)	2.55×10^{-4}	1.06×10^{-4}	2.40
PBDB-T:M1 (CF treated)	1.90×10^{-4}	1.41×10^{-4}	1.34
PBDB-T:M1 (CB treated)	2.81×10^{-4}	2.25×10^{-4}	1.24

12. Morphology and Microstructure Analysis for Blend Films

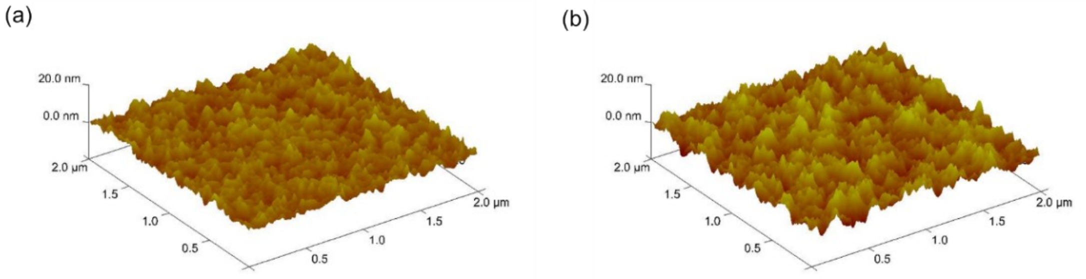

Fig. S14 The AFM three-dimensional images of PBDB-T:SPA-1 blend films (a) treated with CF and (b) treated with CB.

13. ^{1}H NMR Spectra, ^{13}C NMR Spectra and MALDI-TOF-MS Spectra

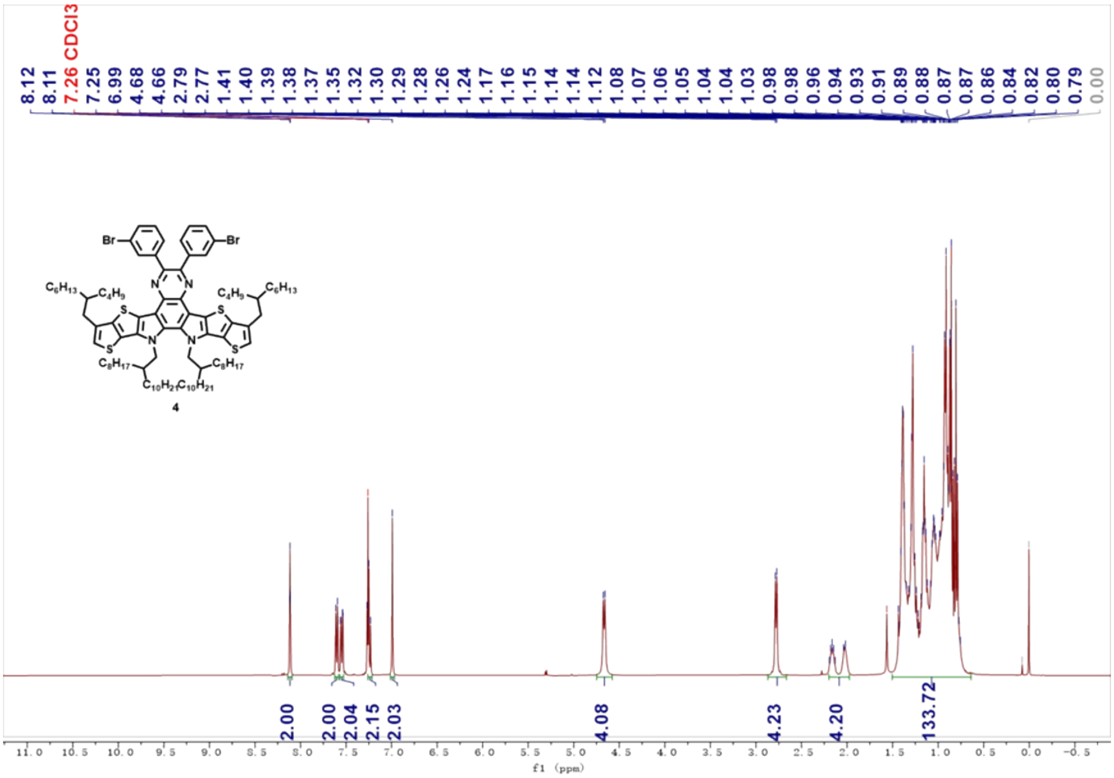

Fig. S15 ^{1}H NMR of compound **4** in $CDCl_3$.

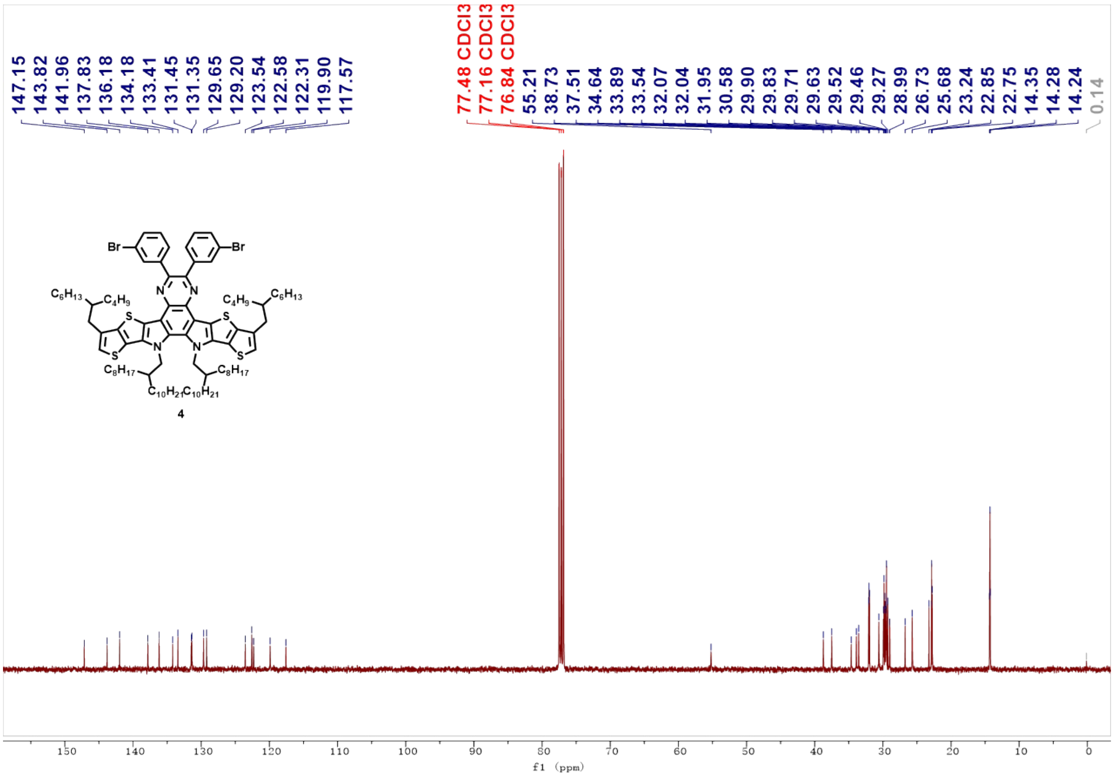

Fig. S16 ^{13}C NMR of compound **4** in $CDCl_3$.

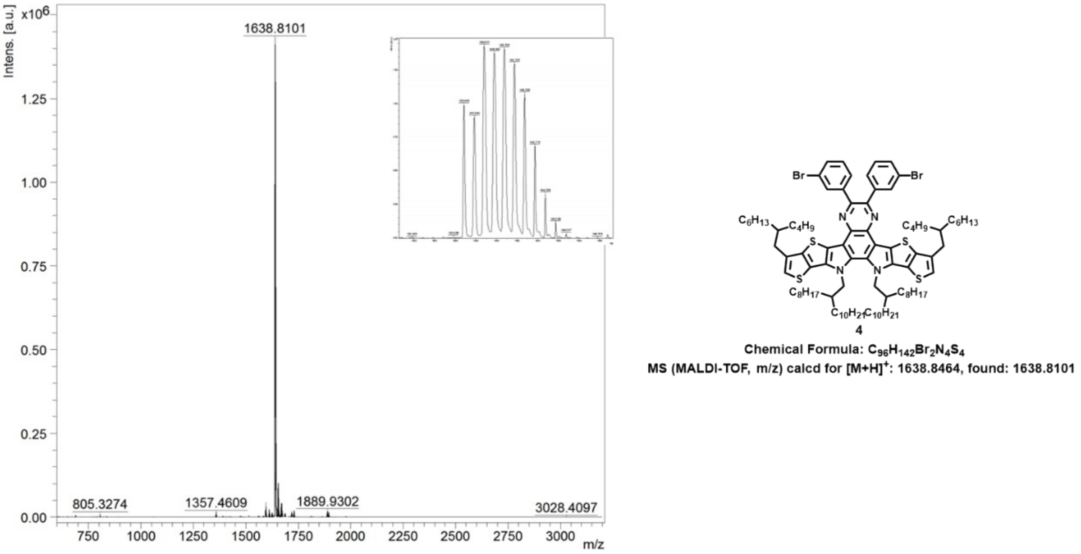

Chemical Formula: $C_{96}H_{142}Br_2N_4S_4$

MS (MALDI-TOF, m/z) calcd for $[M+H]^+$: 1638.8464, found: 1638.8101

Fig. S17 MALDI-TOF-MS of compound **4**.

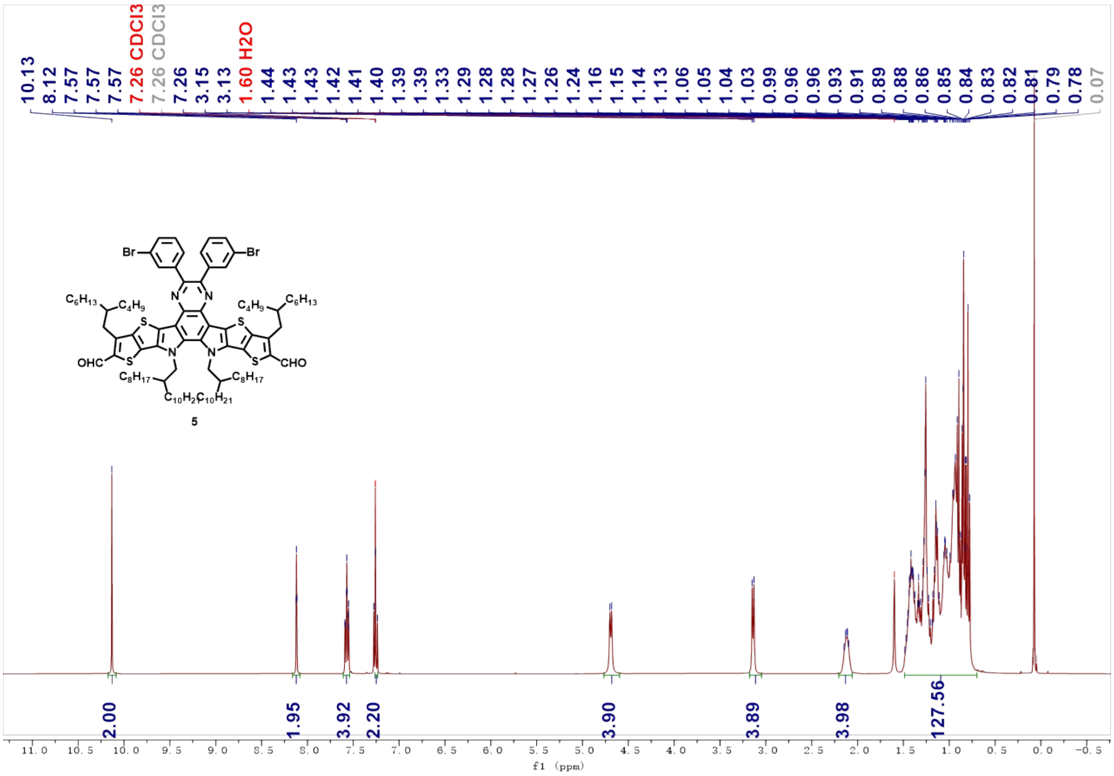

Fig. S18 ^{1}H NMR of compound **5** in $CDCl_3$.

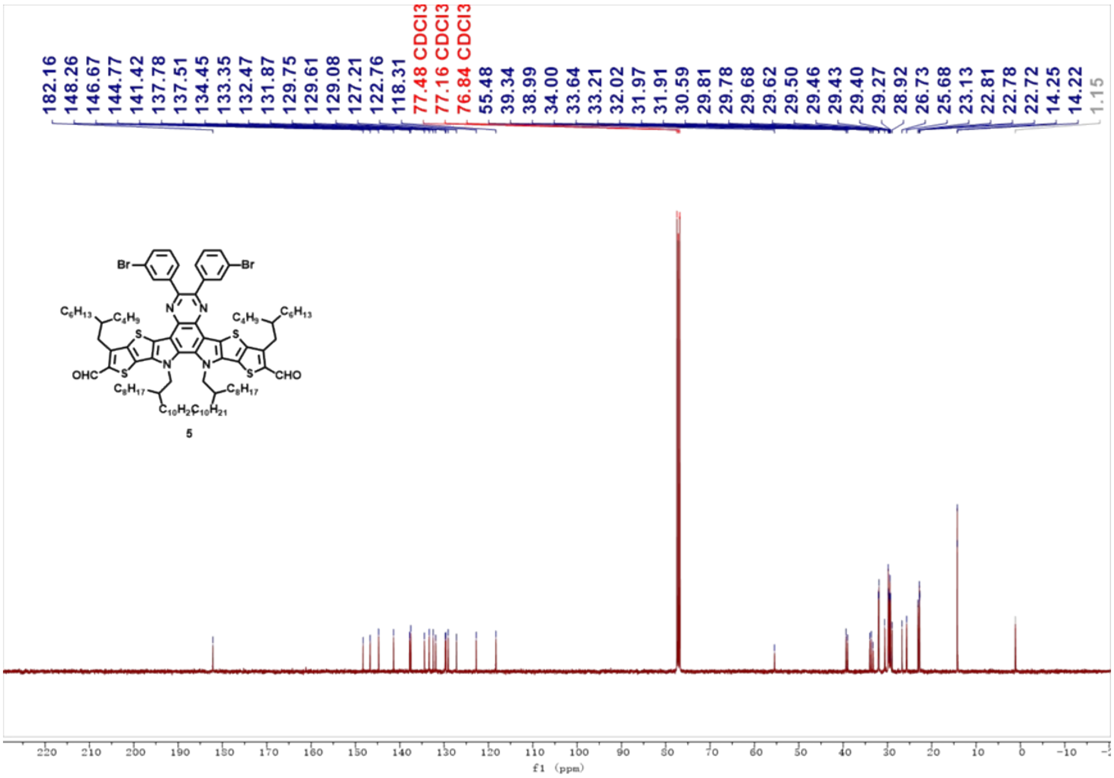

Fig. S19 ^{13}C NMR of compound **5** in $CDCl_3$.

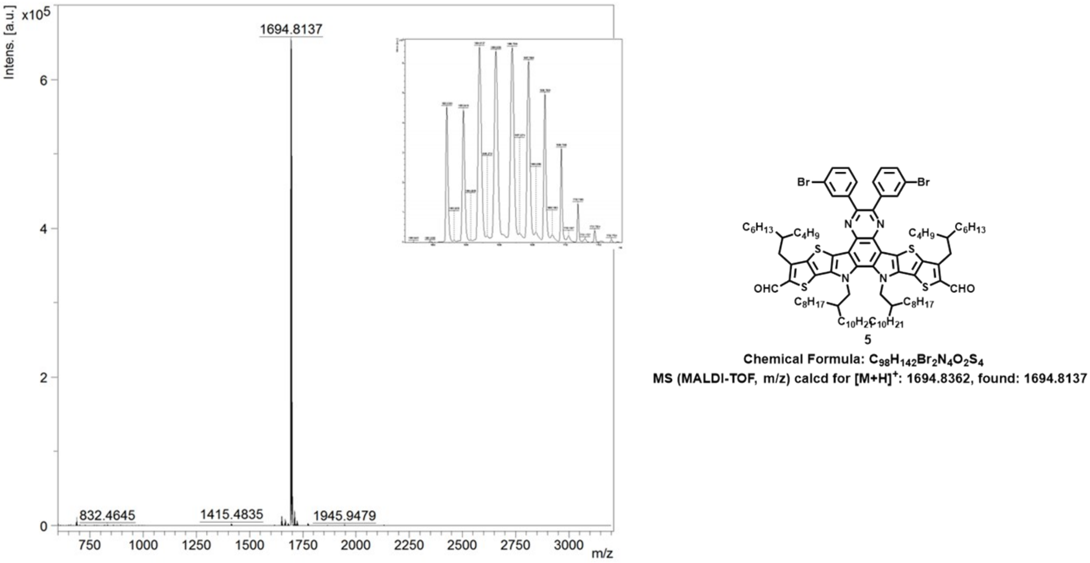

Chemical Formula: $C_{98}H_{142}Br_2N_4O_2S_4$

MS (MALDI-TOF, m/z) calcd for $[M+H]^+$: 1694.8362, found: 1694.8137

Fig. S20 MALDI-TOF-MS of compound **5**.

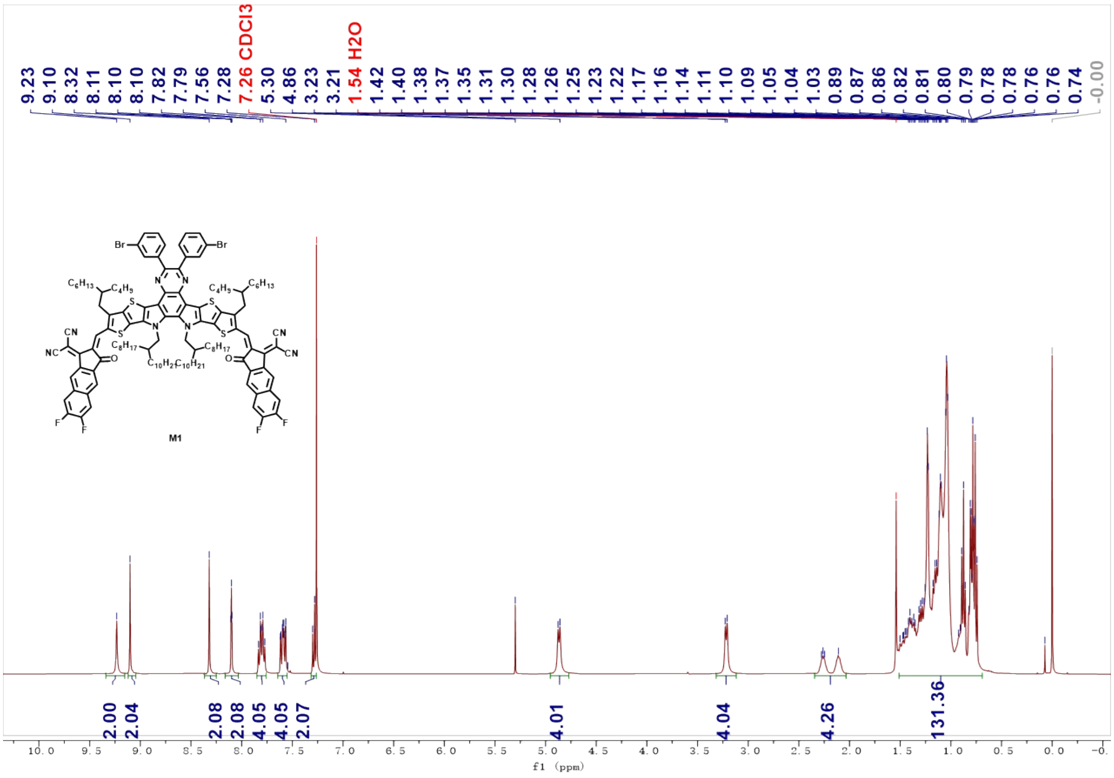

Fig. S21 ^{1}H NMR of compound M1 in $CDCl_3$.

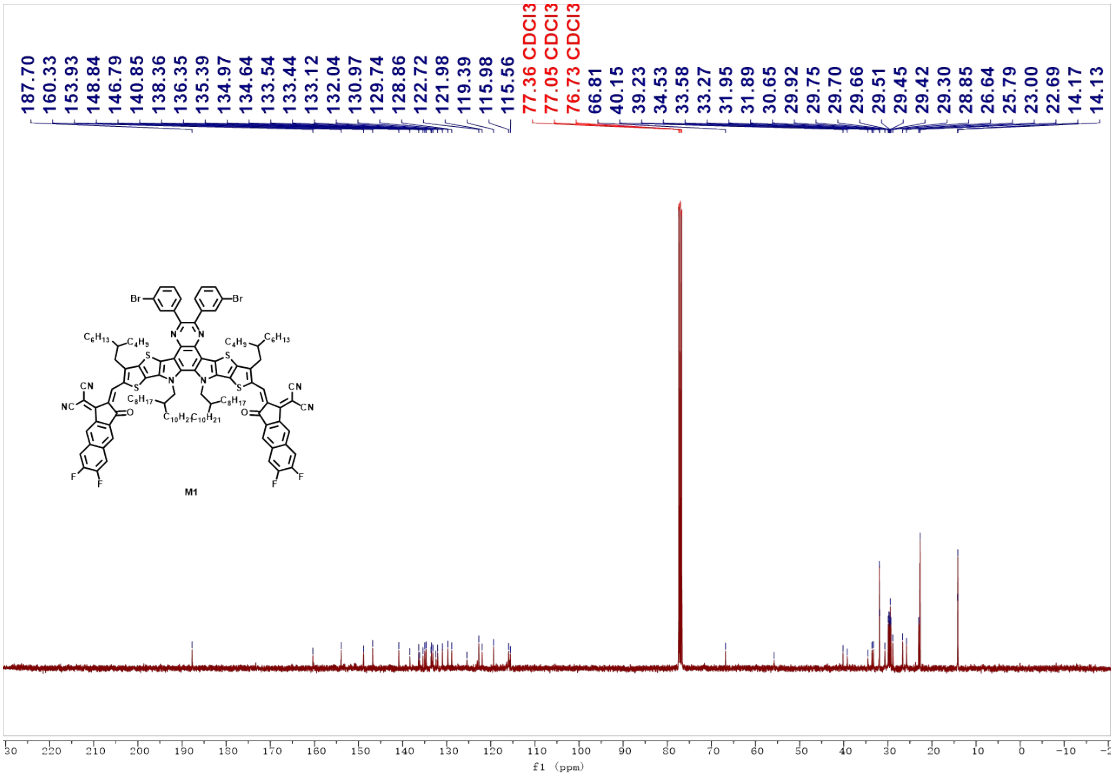

Fig. S22 ^{13}C NMR of compound M1 in $CDCl_3$.

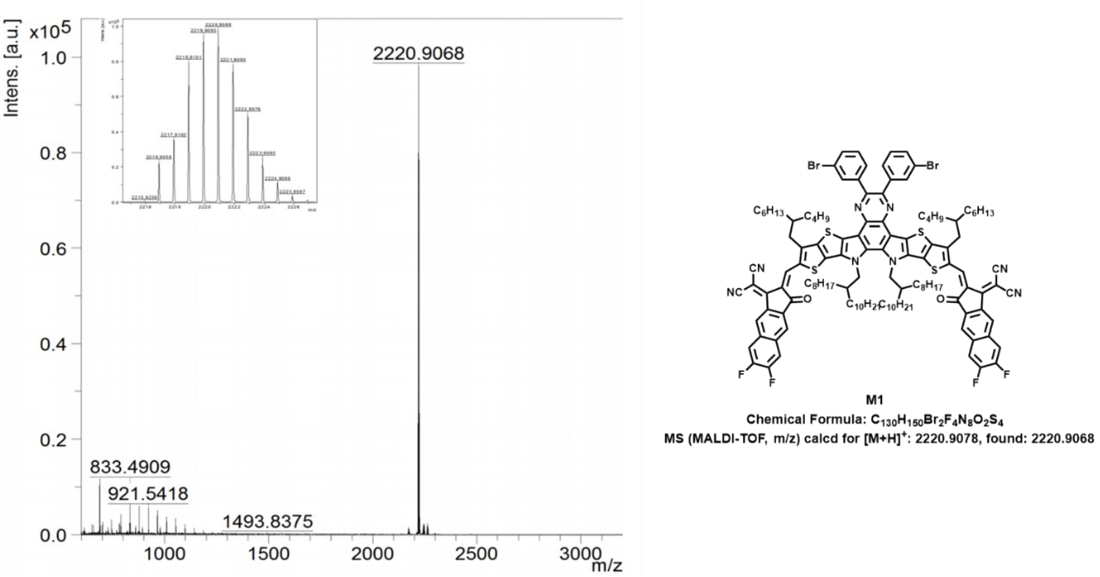

M1

Chemical Formula: $C_{130}H_{150}Br_2F_4N_8O_2S_4$

MS (MALDI-TOF, m/z) calcd for $[M+H]^+$: 2220.9078, found: 2220.9068

Fig. S23 MALDI-TOF-MS of M1.

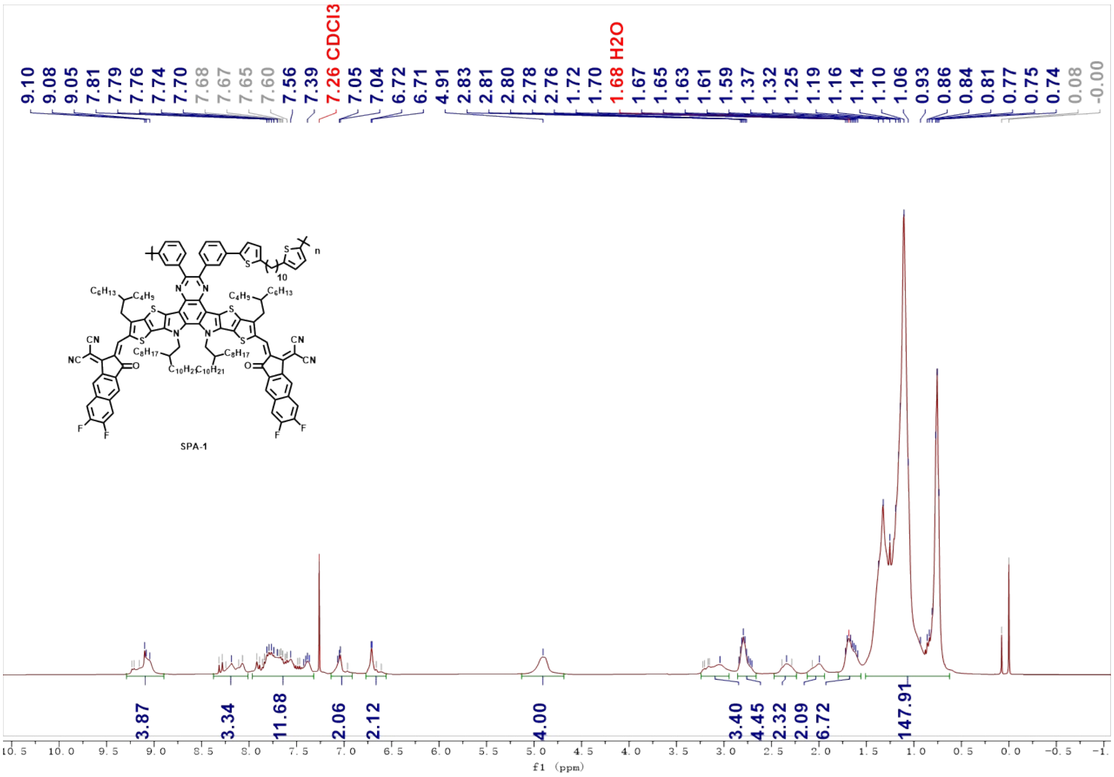

Fig. S24 ^{1}H NMR of non-conjugated polymer acceptor SPA-1 in $CDCl_3$.

References

1. C. Plett and S. Grimme, *Angewandte Chemie International Edition*, 2023, **62**, e202214477.
2. S. Spicher and S. Grimme, *Angewandte Chemie International Edition*, 2020, **59**, 15665-15673.
3. C. Bannwarth, E. Caldeweyher, S. Ehlert, A. Hansen, P. Pracht, J. Seibert, S. Spicher and S. Grimme, *WILEY INTERDISCIPLINARY REVIEWS-COMPUTATIONAL MOLECULAR SCIENCE*, 2021, **11**, e01493.
4. J.-W. Lee, C. Sun, S.-W. Lee, G.-U. Kim, S. Li, C. Wang, T.-S. Kim, Y.-H. Kim and B. J. Kim, *Energy & Environmental Science*, 2022, **15**, 4672-4685.
5. Q. Fan, R. Ma, T. Liu, J. Yu, Y. Xiao, W. Su, G. Cai, Y. Li, W. Peng, T. Guo, Z. Luo, H. Sun, L. Hou, W. Zhu, X. Lu, F. Gao, E. Moons, D. Yu, H. Yan and E. Wang, *Science China Chemistry*, 2021, **64**, 1380-1388.
6. X. Wu, X. Hao, P. Deng and H. Chen, *Dyes and Pigments*, 2021, **196**, 109824.
7. J. Zhang, C.-H. Tan, K. Zhang, T. Jia, Y. Cui, W. Deng, X. Liao, H. Wu, Q. Xu, F. Huang and Y. Cao, *Advanced Energy Materials*, 2021, **11**, 2102559.
8. D. Chen, S. Liu, X. Hu, F. Wu, J. Liu, K. Zhou, L. Ye, L. Chen and Y. Chen, *Science China Chemistry*, 2022, **65**, 182-189.
9. Z. Genene, J.-W. Lee, S.-W. Lee, Q. Chen, Z. Tan, B. A. Abdulahi, D. Yu, T.-S. Kim, B. J. Kim and E. Wang, *Advanced Materials*, 2022, **34**, 2107361.
10. Q. Chen, Y. H. Han, L. R. Franco, C. F. N. Marchiori, Z. Genene, C. M. Araujo,

J.-W. Lee, T. N.-L. Phan, J. Wu, D. Yu, D. J. Kim, T.-S. Kim, L. Hou, B. J. Kim and E. Wang, *Nano-Micro Letters*, 2022, **14**, 164.

11. H. Hu, W. Zhou, J. Liu, J. Xie, S. You, S. Young Jeong, H. Young Woo, F. Wu and L. Chen, *Chemical Engineering Journal*, 2024, **491**, 152009.
12. F. Qin, G. Li, Y. Liu, Y. Cho, R. M. Pankow, D. Zhang, L. Feng, Y. Wang, S. Jeong, G. Forti, D. Zheng, C. Yang, Y. Zhou, T. J. Marks and A. Facchetti, *ACS Energy Letters*, 2023, **8**, 4733-4745.
13. Q. Fan, W. Su, S. Chen, T. Liu, W. Zhuang, R. Ma, X. Wen, Z. Yin, Z. Luo, X. Guo, L. Hou, K. Moth-Poulsen, Y. Li, Z. Zhang, C. Yang, D. Yu, H. Yan, M. Zhang and E. Wang, *Angewandte Chemie International Edition*, 2020, **59**, 19835-19840.
14. J. Liu, J. Deng, Y. Zhu, X. Geng, L. Zhang, S. Y. Jeong, D. Zhou, H. Y. Woo, D. Chen, F. Wu and L. Chen, *Advanced Materials*, 2023, **35**, 2208008.
15. J. Liu, J. Liu, J. Deng, B. Huang, J. Oh, L. Zhao, L. Liu, C. Yang, D. Chen, F. Wu and L. Chen, *Journal of Energy Chemistry*, 2022, **71**, 631-638.
16. J.-W. Lee, S.-W. Lee, J. Kim, Y. H. Ha, C. Sun, T. Ngoc-Lan Phan, S. Lee, C. Wang, T.-S. Kim, Y.-H. Kim and B. J. Kim, *Journal of Materials Chemistry A*, 2022, **10**, 20312-20322.
17. W. Su, Q. Fan, I. Jalan, Y. Wang, W. Peng, T. Guo, W. Zhu, D. Yu, L. Hou, E. Moons and E. Wang, *ACS Applied Materials & Interfaces*, 2021, **13**, 6442-6449.
18. J. Huang, X. Shi, X. Wang, H. Zheng, Y. Fang, Y. Cheng, S. Y. Jeong, H. Y. Woo, Q. Zong and B. Huang, *Chemical Communications*, 2025, **61**, 5142-5145.